A chiral link between structure and magnetism in MnSi

2012 J. Phys.: Condens. Matter 24 366005

(http://iopscience.iop.org/0953-8984/24/36/366005)

IOP PUBLISHING JOURNAL OF PHYSICS: CONDENSED MATTER
J. Phys.: Condens. Matter **24** (2012) 366005 (7pp) doi:10.1088/0953-8984/24/36/366005

A chiral link between structure and magnetism in MnSi

V Dmitriev[1], D Chernyshov[1], S Grigoriev[2] and V Dyadkin[1]

[1] Swiss–Norwegian Beamlines at ESRF, BP 220, Grenoble, F-38043, France
[2] Petersburg Nuclear Physics Institute, Gatchina, 188300 St Petersburg, Russia

E-mail: dmitriev@esrf.fr

Received 30 July 2012
Published 21 August 2012
Online at stacks.iop.org/JPhysCM/24/366005

Abstract
We consider crystal and magnetic chiral structures for MnSi and isostructural metal silicides, where a complete set of structural and magnetic measurements allows us to define both magnetic and structural chiral configurations. We show that magnetic symmetry inherits chirality from the crystal structure. We derive, with emphasis on symmetry arguments, a new type of magneto-structural relation, namely a symmetrized coupling between structural and magnetic chiralities that provides a structural control on the magnetic chirality.

S Online supplementary data available from stacks.iop.org/JPhysCM/24/366005/mmedia

1. Introduction

A chiral structure is a spatial distribution of charge or spin density that does not coincide with its mirror image after any combination of rotations and translations. A chiral medium is optically active and rotates the polarization of light; a magnetic field also affects optical activity. A link between the two phenomena is called magneto-chiral dichroism [1]. This effect promises new control over magnetic properties and is expected to be enhanced in molecular magnets if both crystal and magnetic structures are chiral [2]. However, even for an enantiopure chiral crystal, the relationship between crystallographic and magnetic chiralities is not definitely established. First, chiral magnetic structures have been observed for non-chiral crystals, where magnetic spirals in Ho (space group $P6_3/mmc$) may serve as an example [3].

Second, for many magnetic materials, even if they are crystallized in a chiral space group, their absolute structure cannot be measured with polarized light but requires a special single crystal x-ray diffraction experiment at the wavelength providing significant resonant contribution to violate Friedel's law [4]; most chiral magnetic materials have not been tested in this way so far. Finally, the absolute configuration of a magnetic structure also has to be defined with the help of polarized neutrons, either with small angle diffraction [5, 6] or with spherical neutron polarimetry [7]; neither option is widely available yet.

The symmetry of a crystal allows for chirality only if the space group does not contain symmetry elements of the second kind—inversion, rotoinversions, and mirror planes [4]. Symmetry also provides a link between structure and magnetism, via corresponding coupling terms in the phenomenological expressions for the free energy. Here we explore this link for a chiral crystal structure where magnetic structure is stabilized by Dzyaloshinskii–Moriya interaction. More specifically, we focus on $Mn_xFe_{1-x}Si$ and isostructural $Fe_xCo_{1-x}Si$ compounds where a complete set of structural and magnetic measurements allows us to define both magnetic and structural absolute configurations [6, 8]. The handedness of the magnetic helix (the magnetic chiral structure found for MnSi) has been recently correlated with chiral crystal structure [8, 9]. The correlation has been proved experimentally on a limited number of crystals; here we support these findings with theoretical arguments and show that correspondence between two chiral structures is a general consequence of the symmetry. We show, in agreement with experiment, a new type of magneto-structural relation, namely symmetrized coupling between structural and magnetic chirality that enables structural control on magnetic properties recently reported in [9].

The paper is organized as follows. First, we review the crystal structure and symmetry of MnSi. Then we analyse new symmetries appearing on deformation of the Mn sublattice; we introduce an archetypal symmetry needed for proper phenomenological expression for the free energy, and define

the structural chirality. Magnetic chirality and the coupling with the structural chirality are discussed in the next part, followed by a conclusion.

2. Crystallographic structure and its chirality

2.1. Crystal structure

Pure MnSi, FeSi, their solid solutions and analogues doped with Co belong to the B20 structural type with the space group $P2_13$ [6, 9, 10]; this group does not contain symmetry operations of the second kind and therefore corresponds to a chiral crystal structure. Both transition metal and silicon atoms occupy Wyckoff position 4a:

$$\begin{aligned} 4(\mathrm{a}) : \mathrm{R}_1(u, u, u); \\ \mathrm{R}_2\ (0.5 + u, 0.5 - u, -u); \\ \mathrm{R}_3\ (-u, 0.5 + u, 0.5 - u); \\ \mathrm{R}_4\ (0.5 - u, -u, 0.5 + u) \end{aligned} \qquad (1)$$

with $u = 0.113\,05(10)$ for Mn and $u = 0.4044(2)$ for Si, or $u = 0.887\,04(16)$ for Mn and $u = 0.5954(3)$ for Si (atomic positions are taken from crystallographic data collected for crystals discussed in [9]). These two sets of coordinates are characteristic for two enantiomeric structures that could be transformed one into another by inversion.

It is worth noting that in the literature one finds different numberings for the positions R_1–R_4 in the B20 structure. This variety reflects the orientation ambiguities due to lower point symmetry of the structure as compared with the lattice [11]. In order to provide a unifying reference we use hereafter a standard setup from the International Tables for X-ray Crystallography [12]. The value found in the literature for MnSi, $u = 0.137$–0.138 for Mn, corresponds to $u = 0.113$–0.112 in our setting.

The unit cells can easily be imagined by setting the Me–Si pairs into the fcc lattice sites but orienting these motifs along ⟨111⟩ axes at four different sites [0, 0, 0], [0.5, 0.5, 0], [0, 0.5, 0.5], and [0.5, 0, 0.5]. A convenient, albeit not unique, way to illustrate the difference between two enantiomers is an inspection of a helix propagating along ⟨111⟩ and built from Mn or Si atoms; two structures have helices of opposite sense.

The transition metal atoms forming a helix are skewing around ⟨111⟩ in the left-handed configuration for $u = 0.113\,05(10)$ and in the right-handed configuration for $u = 0.887\,04(16)$. The Si atoms form a similar, but left-handed, helix around ⟨111⟩, in accordance to its parameter $u_{\mathrm{Si}} = 0.5954(3)$, and the right-handed configuration for $u_{\mathrm{Si}} = 0.4044(2)$.

As expected for a chiral structure, two enantiomers cannot be superimposed by a rotation, translation or any combination of these two operations. Two enantiomers can be transformed one to another by inversion, and the corresponding transformation is given by $[-1\,0\,0, 0\,-1\,0, 0\,0\,-1]$; for a single sublattice of Mn or Si this transformation simply implies change of u to $(1 - u)$ in equation (1). In order to distinguish between two structures we call them 'left' and 'right' according to the sense of spiral propagating along ⟨111⟩ and built from silicon atoms.

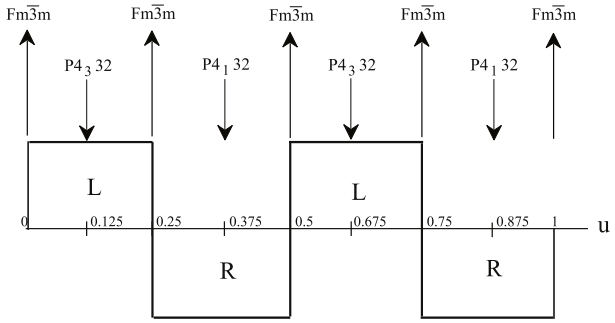

Figure 1. Symmetry of a single sublattice in the B20 structure as a function of atomic position (u, u, u). L and R stand for left- and right-handed versions according to the definition given in the text. Arrows indicate values where symmetry differs from $P2_13$.

2.2. A structural archetype for the B20 structure

For a single sublattice, Mn or Si, the symmetry depends on the parameter u (figure 1). As we have seen in section 2.1, u and $(1 - u)$ correspond to $P2_13$ domains of the opposite chirality. It is easy to see that $u = 0$, 0.25, 0.5, 0.75 form a structure with $Fm\bar{3}m$ symmetry; this is the B2 structure type. It can be also shown, by using equation (1) and analysing the corresponding arrangement of atoms, that $u = 0.125$ (0.325) sets $P4_332$ ($P4_132$) symmetry; notably, these two groups correspond to structures of the opposite chirality. A relation between all these symmetries can be readily found with help of an archetypal structure that would also link phenomena of a different nature observed for a crystal.

Among all possible structures listed above, the hypothetical B2 structure has the highest symmetry and, therefore, can be considered as an archetype for B20 crystals. The archetype consists of two interpenetrating face-centred cubic (fcc) sublattices (Wyckoff positions 4(a) and 4(b) for $Fm\bar{3}m$) filled by different atoms. In our case, one of them contains magnetic atoms (Mn or disordered mixtures like Fe/Co or Mn/Fe); the other one is a non-magnetic Si sublattice.

Without loss of generality, let us focus on the magnetic metal counterpart. A straightforward group-theoretical procedure which starts from the archetypal symmetry $Fm\bar{3}m$ allows us to conclude that a conjectural phase transition $Fm\bar{3}m$ ($Z = 1$) to $P2_13$ ($Z = 4$) (here Z is the number of formula units in a *primitive* but not Bravais unit cell), corresponding to the B2 to B20 structural phase transition, would be induced by a six-component order parameter (OP) (see, for example, [13]). The OP belongs to the point X (three-armed vector star $\mathbf{k}^{(1)} = (\mathbf{b}_1 + \mathbf{b}_2)/2$) of the face-centred Brillouin zone (BZ), it spans six-dimensional irreducible representation X_5^-.

The relevant mechanical (displacive) representation M of $Fm3m$ should be constructed at the X point of the BZ and on the site positions of the fcc lattice, i.e. positions (1) with $u = 0$,

$$\begin{aligned} 1 : (0, 0, 0,); \qquad & 2 : (0.5, 0.5, 0); \\ 3 : (0, 0.5, 0.5); \qquad & 4 : (0.5, 0, 0.5). \end{aligned} \qquad (2)$$

It reduces to two irreducible representations, $M_{(a)} = X_2^- + X_5^-$, which correspond to longitudinal (LO) and transverse (TO) optical phonons, respectively. The basis functions for the three-dimensional X_2^- and six-dimensional X_5^- are:

$$\begin{aligned} X_2^- : \boldsymbol{\psi}_1 &= \mathbf{z}_1 + \mathbf{z}_2 - \mathbf{z}_3 - \mathbf{z}_4, \\ \boldsymbol{\psi}_2 &= \mathbf{y}_1 - \mathbf{y}_2 - \mathbf{y}_3 + \mathbf{y}_4, \\ \boldsymbol{\psi}_3 &= \mathbf{x}_1 - \mathbf{x}_2 + \mathbf{x}_3 - \mathbf{x}_4; \\ X_5^- : \boldsymbol{\varphi}_1 &= \mathbf{x}_1 + \mathbf{x}_2 - \mathbf{x}_3 - \mathbf{x}_4, \\ \boldsymbol{\varphi}_2 &= \mathbf{y}_1 + \mathbf{y}_2 - \mathbf{y}_3 - \mathbf{y}_4, \\ \boldsymbol{\varphi}_3 &= \mathbf{z}_1 - \mathbf{z}_2 - \mathbf{z}_3 + \mathbf{z}_4, \\ \boldsymbol{\varphi}_4 &= \mathbf{x}_1 - \mathbf{x}_2 - \mathbf{x}_3 + \mathbf{x}_4, \\ \boldsymbol{\varphi}_5 &= \mathbf{y}_1 - \mathbf{y}_2 + \mathbf{y}_3 - \mathbf{y}_4, \\ \boldsymbol{\varphi}_6 &= \mathbf{z}_1 - \mathbf{z}_2 + \mathbf{z}_3 - \mathbf{z}_4 \,. \end{aligned} \tag{3}$$

Here $\mathbf{x}_i$, $\mathbf{y}_i$ and $\mathbf{z}_i$ are projections of the displacements for the atom number i from (2).

The distortions induced by the OP X_5^- in the phase $P2_13$ are identified by the following relations between the OP components η_ι (see, for example, [13], and supplementary material available at stacks.iop.org/JPhysCM/24/366005/mmedia, equation (1)):

$$\begin{aligned} &\eta_1 = \eta_3 = \eta_5 \neq 0 \leftrightarrow \varphi_1 = \varphi_3 = \varphi_5 \neq 0 \\ &\eta_2 = \eta_4 = \eta_6 = 0 \leftrightarrow \varphi_2 = \varphi_4 = \varphi_6 = 0. \end{aligned} \tag{4}$$

The relations in (4) minimize the corresponding free energy and stabilize the B20 structure. Combining equations (3) and (4), one finds that the shifts of all atoms in the distorted $P2_13$ structure are equal: $x_i = y_j = z_k = u$ (i, j, k are from 1 to 4). Thus, the relevant transformation mechanism consists of symmetrized combinations of atomic displacements which have the same symmetry properties as eigenvectors of TO phonons in the X point of the BZ (figure 2). However, at variance with a displacive transition induced by a soft mode, the atomic displacements are not small. Moreover, the transformation between the archetypal B2 structure and the one corresponding to the special value $u = 0.125$ is of a reconstructive type because for its space groups $Fm\bar{3}m$ and $P4_332$ (or $P4_132$) there is no group–subgroup relation.

2.3. Phase transitions in the B2 structure

Let us follow the phenomenological scheme developed earlier for the displacive reconstructive phase transitions [14, 15], which are specified by non-small atomic shifts breaking the group–subgroup relationship for neighbouring phases. The order parameter was shown to be a periodic function of the atomic displacements [14], and we can deduce a similar function for the X_5^- OP, which should express the periodic distortion of the archetypal fcc structure as a function of the magnitude of the displacements u (see equation (1)).

The conditions on the OP components established by equation (4), which minimize the free energy, significantly simplify our task. First, the equality of three OP components allows us to introduce only one scalar variable parameter $\eta = \eta_1 = \eta_3 = \eta_5$ which is now an effective OP. Second, the

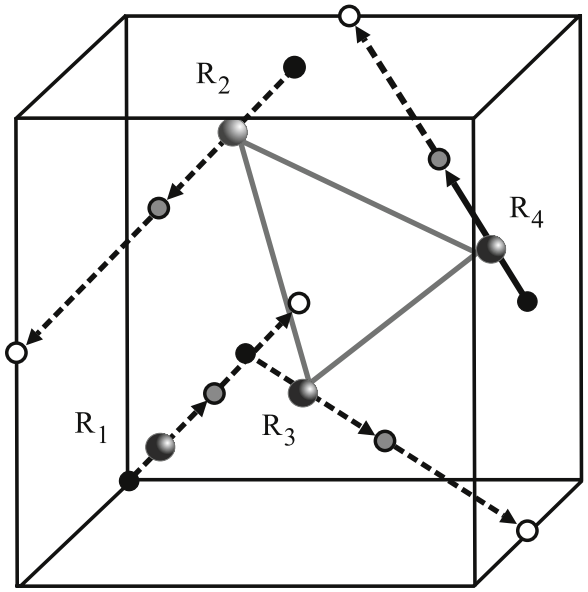

Figure 2. Order parameter for the B2–B20 structural transformation seen for the magnetic metal sublattice. Full and open circles correspond to the B2 structure ($u = 0.0$ and 0.25). Grey circles represent the B20 structure (numbering of atoms is in accordance with equation (1)). Positions of atoms at $u = 0.125$ are shown as greyish-filled circles.

corresponding equality of the basis functions $\varphi_1 = \varphi_3 = \varphi_5$ fixes the directions of atomic displacements to the $\langle 111 \rangle$-type and reduces the set of vector variables to a scalar u. This is the modulus of the corresponding displacement vector $\Delta\mathbf{r}_i = \mathbf{n}_i \cdot u$, where $\mathbf{n}_i$ is a unit vector in the direction $\langle 111 \rangle$.

Following a general procedure [15], after subtraction of the density wave corresponding to atomic planes in the distorted structure from that in the parent B2 structure, we obtain the following periodic function

$$\eta(u) = A \sin(4\pi u), \tag{5}$$

where η is the above defined effective phenomenological OP and A is a normalizing coefficient. Figure 3 shows the antiparallel shifting mechanism in one of the sublattices of B2 corresponding to OP X_5^- whose magnitude is defined by the periodic function (5).

One sees that the parent B2 structure corresponds to $u = 0$, 0.25, 0.5, 0.75, positions where $\eta = 0$ in accordance with the OP definition. Magnitudes of displacement $u = 0.125$, 0.375, 0.675, ... correspond to a new structure characterized by the equidistant arrangement of the split atomic planes. Its space group $P4_332$ (or $P4_132$) ($Z = 4$) is not a subgroup of $Fm\bar{3}m$ ($Z = 1$). For all other displacements, the structure of the crystal is lowered to the B20 structure (space group $P2_13$), which corresponds to the maximal sub-structure common to $Fm\bar{3}m$ and $P4_332$ structures (figure 1).

Let us emphasize that the above consideration is equally valid for both fcc sublattices and, therefore, for the entire B2 structure. This formal transformation scheme provides a necessary basis for analysing variations of the structure and magnetic chirality in B20 compounds.

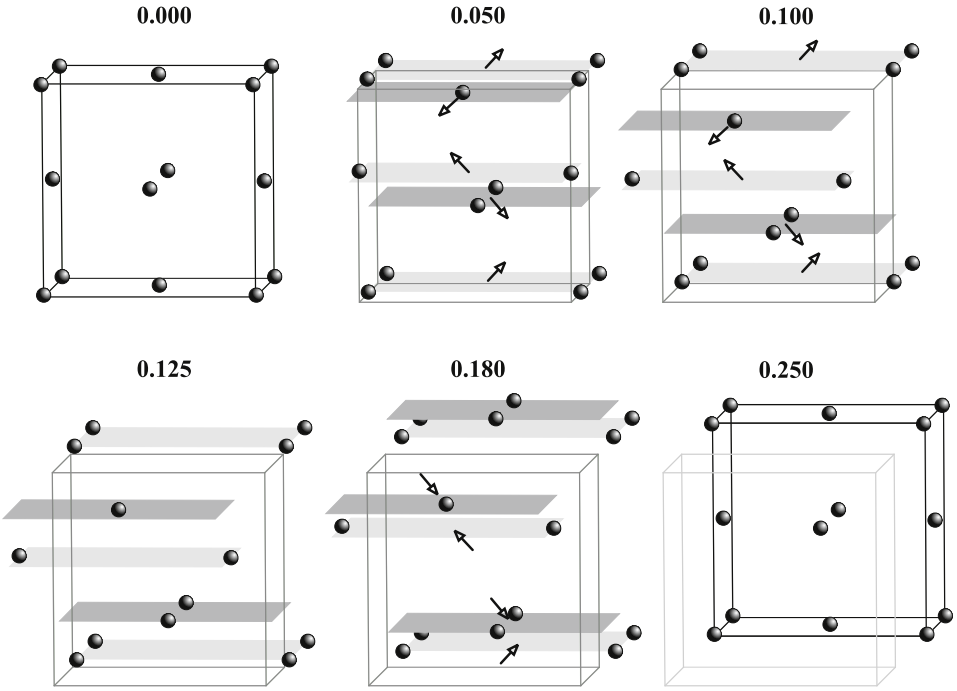

Figure 3. Antiparallel displacement mechanism which leads from the $Fm\bar{3}m$ structure ($u = 0.000$) to $P4_332$ ($u = 0.125$). The figure with $u = 0.250$ represents an antiphase domain of the $Fm\bar{3}m$ parent structure.

2.4. Chirality of the crystal structure

In recent combined single crystal neutron scattering and x-ray diffraction experiments [6, 8], it was shown that the sense of the spin helix in MnSi and $Fe_{1-x}Co_xSi$ compounds correlates with the absolute crystal structure. In order to parameterize the coupling between magnetic and structure chiralities, we define in the following structural chirality not as a property but as a parameter.

In earlier publications, several definitions have been introduced for the chirality. Imposing no intrinsic contradictions, vector, pseudo-vector and pseudoscalar values were used for characterizing different properties of chiral systems. The choice is predetermined by the goal: whether one focuses on structural effects (the (pseudo)vector characteristic of a helix is sufficient), or one aims to discuss the free energy of a system and the coupling of chiral effects of different natures (pseudoscalar chirality is appropriate). Our consideration falls to the latter category.

It is well understood that structures belonging to space groups that lack inversion centres, reflection planes, glide planes or rotatory-inversion axes can contain chiral objects. On the one hand, these latter can be chiral molecules, and their proper chirality predetermines the chirality of the crystal structure. On the other hand, even in a system of non-chiral atoms and ions fragments with a chiral structure can be built up. A tutorial example is structure of two chiral twin domains of α-quartz with $P3_121$ and $P3_221$ symmetry. It can be related to $P6_422$ and $P6_222$ domains of the high temperature β-quartz; chirality has therefore been retained in the phase transition between two quartz polymorphs. In contrast, the transition between B2 and B20 structures related via X_5^- OP is a transition between achiral and chiral structures, thus assuming that corresponding OP should assure the property of chirality. Figure 4 shows the arrangement of the original fcc sublattice of magnetic atoms in the three cubic structures: the parent B2 ($u = 0.000$), and two distorted $P2_13$ domains, corresponding to the different signs of the OP η ($u = 0.050$ and -0.050).

One can see that, depending on the sign of OP, the shifted atoms are organized in either right-handed or left-handed helices. It should be specially emphasized that the four atoms enumerated in (1) and shown in figure 2 constitute flat triangles having no chiral arrangement. The helices are built up with atoms belonging to different triangles from different cubic unit cells (figure 4). The helices, therefore, fill one of the triangular prisms, containing either a screw three-fold axis 3_1 or $3_2 = 3_1^-$ of the corresponding space group, the other prism remaining empty. Thus, the structures distorted towards a closer, denser surrounding of certain screw rotation axes show disproportion of partial chiralities of different signs. It should be noted, however, that in the framework of the formal geometry the entire crystal structure does not show any 'disequilibria' as both the symmetry elements, clockwise rotation 3_1 and anti-clockwise $3_2 = 3_1^-$, act on the space group positions. However, in physical consideration of real structures, the above difference in the atomic arrangement might play a crucial role.

We define the integral chirality of a sublattice (structure) as a sum of the partial chiralities of atomic configurations confined in two cell prisms (figure 4):

$$h_S = h_S^+ + h_S^-, \tag{6}$$

where the sign '+' or '−' coincides with the sign of the shifts in equation (1) or, in the other terms, with the sign of the

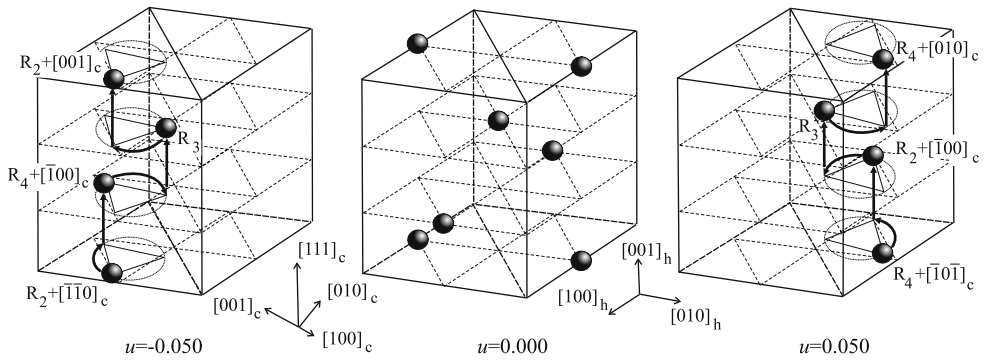

Figure 4. Hexagonal (h) setting of cubic (c) structures $P2_13$ ($u = 0.050$ and -0.050) and $Fm\bar{3}m$ ($u = 0.000$). Numbering of atoms corresponds to equation (1). Vectors $[hkl]_c$ at R_i indicate to which unit cell the corresponding position belongs.

order parameter η (5). The partial chirality we define as a dot product between the axial vector $[\mathbf{R}_{ji} \times \mathbf{R}_{jk}]$ and the unit vector $\mathbf{U}_{[111]}$. Vectors $\mathbf{R}_{ji} = \mathbf{R}_j - \mathbf{R}_i$ (see equation (1)) connect the nearest atoms from sequential layers in the structure (figure 4), and their vector product characterizes the direction of rotation in a helix when going up from a lower to a higher layer. The terms 'lower' and 'higher' are fixed by the direction of $\mathbf{U}_{[111]}$, and the above dot product is a scalar projection of the axial vector on the lattice direction $\langle 111 \rangle$.

In the case of positive shifts u (right panel in figure 4) $h_S^- = 0$ (no atoms in the corresponding prism), and $h_S = h_S^+$:

$$h_S = h_S^+ = \mathbf{U}_{[111]} \cdot [\mathbf{R}_{34} \times \mathbf{R}_{32}]. \tag{7}$$

For negative shifts (left panel in figure 3) $h_S^+ = 0$, and h_S reads:

$$h_S = h_S^- = \mathbf{U}_{[111]} \cdot [\mathbf{R}_{32} \times \mathbf{R}_{34}]. \tag{8}$$

A few properties of h_S are worth noting. First, in full agreement with symmetry properties of chiral objects, the chirality h_S is a pseudoscalar, as it resulted from the dot product of a vector ($\mathbf{U}$) and a pseudo-vector (axial vector $[\mathbf{R}_{ji} \times \mathbf{R}_{jk}]$). Second, in full agreement with our expectations the structure chirality reverses its sign with change of the direction of atomic shifts:

$$\begin{aligned} h_S^+ &= \mathbf{U}_{[111]} \cdot [\mathbf{R}_{jk} \times \mathbf{R}_{ji}] \\ &= -\mathbf{U}_{[111]} \cdot [\mathbf{R}_{ji} \times \mathbf{R}_{jk}] = -h_S^-. \end{aligned} \tag{9}$$

Finally, structure chirality vanishes ($h_S = 0$) in the centrosymmetric parent phase as the atoms are equally present in both the prisms, i.e. $|h_S^+| = |h_S^-|$.

It should be emphasized that the definition in (6)–(8) cannot be used as a quantitative one but reflects only the symmetry properties of the corresponding parameters.

2.5. Order parameter and chirality

Equation (1) and figure 2, on the one hand, and equations (7)–(9), on the other, indicate (see also supplementary material available at stacks.iop.org/JPhysCM/24/366005/mmedia) a functional link between the OP $\eta(u)$ of the B2–B20 structural phase transition and the structure chirality parameter h_S. The relations become even more evident if we look at the same structure distortion along the $\langle 111 \rangle$ cubic direction (figure 5). Figure 1 visualizes the periodic variation of the structural chirality defined by equation (6) and related to filling and emptying triangular prisms (compare to figure 5). Note that the process is fully controlled by the structural OP X_5^-, and it has the same periodicity as the function $\eta(u)$ (see equation (5)). Keeping in mind the above remark on the qualitative character of the definition equations (7)–(9), we could use formally, for characterizing the crystal handedness, the function $h = \mathrm{sgn}[\eta(u)]$ (figure 1) which is positive at $0 < u < 0.25$, and negative for $0.25 < u < 0.50$ (or $-0.25 < u < 0$).

3. Magnetic helix and structural chirality

Theoretical works [16, 17] have shown that the ferromagnetic spiral in MeSi compounds is caused by a Dzyaloshinskii–Moriya interaction which arises because of the non-centrosymmetric arrangement of magnetic atoms in the structure. The Dzyaloshinskii mechanism stabilizing a long-period magnetic superstructure is caused by weak 'relativistic' spin–lattice or spin–spin interactions. It was shown by Moriya that an invariant of the required form can result from antisymmetric microscopic coupling between two localized magnetic moments $\mathbf{S}_i$ and $\mathbf{S}_j$:

$$E_{ij}^{\mathrm{DM}} = \mathbf{D}_{ij} \cdot [\mathbf{S}_i \times \mathbf{S}_j]. \tag{10}$$

In the case of a long-period helical spin density wave the Dzyaloshinskii energy term has the form $D(\mathbf{S} \cdot \nabla \times \mathbf{S})$. Substituting into the latter a periodic function of the spin wave yields that the 'Dzyaloshinskii vector' $\mathbf{D}_{ij}$ is simply its wave propagation vector $\mathbf{k}$ (see [16]). The expression of equation (10) is, therefore, a characteristic parameter of the magnetic chirality of the structure.

Let us underline the similarity in the symmetry properties of two parameters, h_S and E^{DM}, both characterizing chiralities of a different nature and which together should affect the free energy of a B20 structure. Parameters h_S (equations (6)–(9)) and E^{DM} (equation (10)) are both pseudoscalars—dot products between an axial vector and a true vector. It is worth noting a similar structure of the terms (7)–(8) and (10) too:

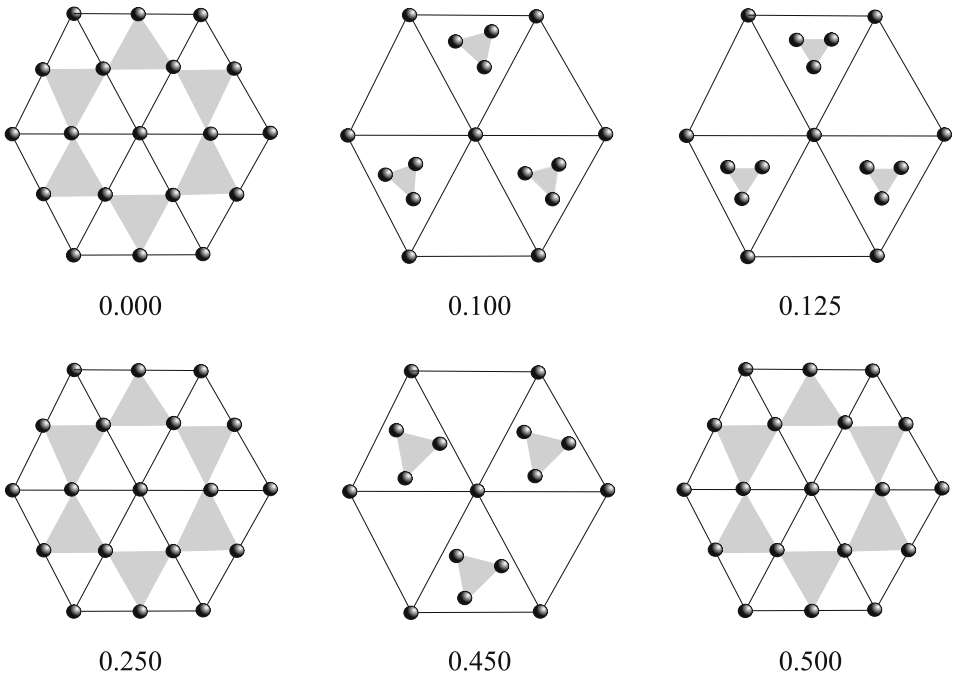

Figure 5. Atomic shifts induced by the order parameter X_5^- in the fcc lattice. The shifts $u = 0.000$, 0.250 and 0.500 correspond to zeros of the function (5); for $u = 0.125$ the structure $P4_332$ (4) breaks the group–subgroup relation with the parent $Fm\bar{3}m$ (1). The view is along the ⟨111⟩ cubic direction.

formally they are scalar projections of a certain density wave on the direction of its propagation.

The evident consequence of the identical symmetry of the chiral parameters is that any hypothetical process acting upon the crystal and characterized by the pseudoscalar symmetry should affect both the structural and the magnetic chiralities at the same time.

The simultaneous variation of the chiralities (both positive or negative, or of different signs) might be also concluded from the free energy consideration. Indeed, either of equations (6) and (10) is an antisymmetric counterpart to symmetric dot products—second-degree terms in the free non-equilibrium energy (Landau potential): the former to a harmonic part of the displacive energy, the latter to the symmetric Heisenberg exchange term in the magnetic energy contribution. Equations (6) and (10) are not invariant in the parent $Fm\bar{3}m$ phase, as they change their sign under inversion; this implies a difference in free energies for two enantiomers if the odd degree of these equations directly contributes to the free energy. However, their bilinear product $(h_S \cdot E^{DM})$ is an invariant under inversion operation. The bilinear coupling means strictly simultaneous change of the coupled parameters; in our case it implies a simultaneous change of the sign for both chiralities. However, if such a change happens, symmetry considerations alone do not allow us to define a driving force—only microscopic theory or experiment can distinguish between primary and secondary effects in the formation of a chiral state.

The other point worth noting is the fact that in terms of the symmetry scheme developed in this paper, the right-handed and left-handed enantiomeric modifications of the B20 structure appear as two equal domains of the same low-symmetry phase, corresponding to different signs of the relevant OP. Indeed, the Landau potential with OP X_5^- contains only even-degree terms (see the corresponding basis of invariants in supplementary material available at stacks.iop.org/JPhysCM/24/366005/mmedia). Thus, the change in the sign of OP does not change the equilibrium energy of the low-symmetry phase, and two distorted structures should be identified as equivalent domains of the same structure.

4. Conclusion

In the paper we analyse the symmetry of metal silicides in order to rationalize a link between structural and magnetic chirality observed experimentally [6, 8, 9]. It is shown that the symmetry of a single metal sublattice possesses periodic changes as a function of displacement of the transition metal atom along the main cubic diagonal. We parameterize these changes in the framework of the phenomenological scheme developed earlier for displacive reconstructive phase transitions. The highest possible parent symmetry is achiral, and its distortion towards chiral low-symmetry forms is described by a corresponding order parameter. We show that such a parameterization necessarily accounts for the chirality, since the latter order parameter changes the sign under inversion; the free energy for two structural domains related by inversion is exactly the same.

For magnetic symmetry which is a subgroup of the structural one, magnetic ordering cannot introduce inversion or mirror operations absent in the crystal symmetry group. Therefore magnetic ordering taking place in the chiral sub-structure should also be chiral. Magnetic chiral structures are also possible in achiral crystal structures if their

magnetic subgroup does not contain second-order symmetry elements, for such a scenario two domains of opposite chirality should be formed having the same energy unless an external perturbation shifts the equilibrium. This was nicely demonstrated earlier for Ho, where equilibrium of two magnetic domains of the opposite chirality can be shifted by an external elastic deformation (torsion) [3].

If magnetic chirality originates not from symmetric but from antisymmetric exchange interactions, the corresponding chiral structure is stabilized by the Dzyaloshinskii–Moriya interaction; this is the source of magnetic chirality in metal silicides. Since the Dzyaloshinskii term is pseudoscalar it has a different sign for two chiral domains related by inversion. Such a difference in energy is not met in the scattering experiments, where two domains are equally present. We propose that the Dzyaloshinskii term contributes to free energy as a bilinear product with the structural chirality; both chiralities have to change sign at the same time under inversion operation. This implies that magnetic chirality is predefined by structural chirality; their ratio depends on the corresponding coupling coefficient. However, the sign of this latter cannot be predicted in the framework of a general phenomenological approach, and therefore one cannot conclude on the signs of two chiralities if they have identical signs or opposite ones. This is a typical problem for microscopic considerations; magnetic chiral structures originating from the Dzyaloshinskii–Moriya interaction have recently been analysed in [18]. The microscopic nature of the phenomenological chiral link between structure and magnetism remains to be revealed; there is a correlation between structural and magnetic chirality and magneto-transport properties first noted in [8]. This correlation indicates that interaction of conduction electrons with localized magnetic moments may play a certain role, at least for metal silicides.

We conclude with a note on experimentation. It was the experimental conclusions about chiral asymmetry in MnSi that largely stimulated our experimental investigations of structural and magnetic chiralities. Such an asymmetry has been expected from the asymmetry of the Dzyaloshinskii–Moriya interaction [19]. We have proved that this asymmetry is not met in reality and both left and right forms could be easily prepared [9]. These conclusions are made possible by a combination of diffraction techniques probing structural and magnetic chirality separately, namely single crystal diffraction of synchrotron radiation and small angle scattering of polarized neutrons. The set of experimental probes could also be further complimented by x-ray magnetic circular dichroism for synchrotron radiation and spherical polarimetry for neutron scattering, that could elucidate the microscopic nature of the chiral interplay between crystallographic structure and magnetic ordering.

References

[1] Rikken G L J A and Raupach E 1997 *Nature* **390** 493
[2] Kishine J, Inoue K and Yoshida Y 2005 *Prog. Theor. Phys. Suppl.* **159** 82
[3] Plakhty V P, Schweika W, Bruckel Th, Kulda J, Gavrilov S V, Regnault L-P and Visser D 2001 *Phys. Rev.* B **64** 100402
[4] Flack H D and Bernardinelli G 2008 *Chirality* **20** 681
[5] Maleyev S V 1995 *Phys. Rev. Lett.* **75** 4682
[6] Grigoriev S V, Chernyshov D, Dyadkin V A, Dmitriev V, Maleyev S V, Moskvin E V, Menzel D, Schoenes J and Eckerlebe H 2009 *Phys. Rev. Lett.* **102** 037204
[7] Poole A, Brown P J and Will A S 2009 *J. Phys.: Conf. Ser.* **145** 01207
[8] Grigoriev S V *et al* 2011 *Phys. Rev.* B **81** 012408
[9] Dyadkin V A, Grigoriev S V, Menzel D, Chernyshov D, Dmitriev V, Schoenes J, Maleyev S V, Moskvin E V and Eckerlebe H 2011 *Phys. Rev.* B **84** 014435
[10] Tanaka M, Takayoshi H, Ishida M and Endoh Ya 1985 *J. Phys. Soc. Japan* **54** 2970
Ishida M, Endoh Ya, Mitsuda S, Ishikawa Y and Tanaka M 1985 *J. Phys. Soc. Japan* **54** 2975
[11] Hostettler M and Flack H D 2003 *Acta Crystallogr.* B **59** 537
[12] Hahn Th (ed) 2006 *International Tables for Crystallography* vol A (Berlin: Springer)
[13] Stokes H T and Hatch M D 1988 *Isotropy Subgroups of the 230 Crystallographic Space Groups* (Singapore: World Scientific)
[14] Dmitriev V, Roshal S, Gufan Y and Toledano P 1988 *Phys. Rev. Lett.* **60** 1958
[15] Toledano P and Dmitriev V 1996 *Reconstructive Phase Transitions in Crystals and Quasicrystals* (Singapore: World Scientific)
[16] Bak P and Jensen M H 1980 *J. Phys. C: Solid State Phys.* **13** L881
[17] Nakanishi O, Yanase A, Hasegawa A and Kataoka M 1980 *Solid State Commun.* **35** 995
[18] Chizhikov V A and Dmitrienko V E 2012 *Phys. Rev.* B **85** 014421
[19] Kishine J, Inoue K and Yoshida Y 2005 *Prog. Theor. Phys. Suppl.* **159** 82